

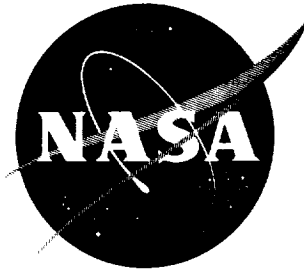
272

N 68 70069

201

NASA TN D-1729

NASA TN D-1729



# TECHNICAL NOTE

D-1729

CALIBRATION OF A THERMAL-CONDUCTIVITY VACUUM GAGE  
IN THE RANGE OF  $10^{-4}$  TO 1 TORR BY MEANS OF  
A VOLUME-RATIO CALIBRATION SYSTEM

By Raymond Holanda

Lewis Research Center  
Cleveland, Ohio

NATIONAL AERONAUTICS AND SPACE ADMINISTRATION  
WASHINGTON

June 1963



NATIONAL AERONAUTICS AND SPACE ADMINISTRATION

---

TECHNICAL NOTE D-1729

---

CALIBRATION OF A THERMAL-CONDUCTIVITY VACUUM GAGE

IN THE RANGE OF  $10^{-4}$  TO 1 TORR BY MEANS OF

A VOLUME-RATIO CALIBRATION SYSTEM

By Raymond Holanda

SUMMARY

Pressure measurements obtained with the thermal-conductivity gage were reproducible to about 1 percent to the lower limit of  $10^{-2}$  Torr and to 2 percent to the lower limit of  $10^{-4}$  Torr. Calibration curves for several gases are presented. Pressures in the range of  $10^{-4}$  to 1 Torr were accurately created by the injection of a small volume of relatively high pressure gas into a large chamber that was initially at substantially zero pressure. An error analysis showed that pressures as low as  $2 \times 10^{-4}$  Torr could be produced with a maximum limit of error of 3 percent; below  $2 \times 10^{-4}$  Torr the limit of error increased linearly to 6 percent at  $10^{-4}$  Torr.

INTRODUCTION

The purpose of the work described herein was to investigate the adaptability of the thermal-conductivity vacuum gage for use as a working standard in the range of  $10^{-4}$  to 1 Torr. Such a device would be useful in the routine calibration of gages in the laboratory, in calibration and comparison of gages in the field, and in field checking of vacuum systems.

Articles on the subject of thermal-conductivity gages date back to 1906. A bibliography of vacuum and low-pressure measurement, which includes the principal work done on thermal-conductivity gages, has recently been published (ref. 1). In this report, primary emphasis is placed on the factors that influence accuracy and reproducibility. These factors are ambient temperature control, stability of wire properties, gas composition as related to accommodation coefficient, contamination effects, and quality of secondary instrumentation.

In order to obtain specified standards of accuracy, it was first necessary to devise a primary standard to create accurately known pressures in this range. The technique chosen was the volume-ratio method because of its simplicity. The availability of a large volume bell jar was an important factor in obtaining the specified accuracies. The technique had been used successfully by previous investigators (refs. 2 to 5). A physical description of the calibration system together with an analysis of its accuracy is presented herein. A vacuum gage design is described for use in the range of  $10^{-4}$  to 1 Torr.

This report is part of a research program in vacuum measurement being conducted at the Lewis Research Center.

## THERMAL-CONDUCTIVITY GAGE

### Principle of Operation

The heat-transfer relation for a heated wire immersed in a gas is represented by

$$Q_{in} = Q_{rad} + Q_{gas} + Q_{cond} \quad (1)$$

If the wire is heated electrically and the pressure is so low that the wire is considered to be in the free-molecule region, equation (1) becomes

$$\underbrace{i^2 R_w}_{\text{Heat input}} \cong \underbrace{\sigma \epsilon_w (T_w^4 - T_a^4) A_s}_{\text{Radiation loss}} + \underbrace{\alpha \left( \frac{\gamma + 1}{\gamma - 1} \right) \sqrt{\frac{R}{T_a M}} A_s (T_w - T_a) p}_{\text{Gas conduction loss}} + \underbrace{2 A_{cs} k \left( \frac{dT}{dx} \right)_{end}}_{\text{End losses}} \quad (2)$$

provided that the end losses are small.

The practical low-pressure limit of the thermal-conductivity gage is reached when the magnitude of the gas conduction term is of the same order as the random variations in the other terms of equation (2). The upper limit of the gage occurs when the continuum region is reached and heat transfer to the gas is independent of pressure. Between the continuum and the free-molecule regions is the slip region, where heat transfer by conduction to the gas remains some function of pressure, although the relation is no longer linear.

Further information on the principles of operation is given in references 6 and 7.

### Choice of Gage Sensing Element

Following is a list of qualities that are considered desirable in a thermal-conductivity gage sensing element to be used for high accuracy measurements:

- (1) Stability of wire properties, such as emittance and surface condition
- (2) High accommodation coefficient and low emittance, which increase the ratio of  $Q_{gas}/Q_{rad}$  at any given pressure and thus permit measurements to lower pressures for a given measuring sensitivity
- (3) Large ratio of wire length to wire diameter, which minimizes end conduction losses and results in a more uniform axial temperature distribution

- (4) Small wire diameter, which results in extending the free-molecule flow conditions to higher pressures
- (5) Sufficient ruggedness for a wide variety of applications
- (6) Commercial availability, so that any number of elements can be obtained without relying on difficult-to-duplicate laboratory constructions

A gage tube that satisfactorily meets these qualifications is described in the following section.

### Description of Gage

The sensing element is a commercial unit, a typical physical description of which is given in table I. The helical wire geometry results in a greater length-diameter ratio for a fixed distance between end supports compared with a straight wire and provides a desirable degree of ruggedness compared with a wire tightly drawn between supports.

The wire is placed in a Wheatstone bridge and is operated at constant wire resistance  $R_w$  and thus constant wire temperature  $T_w$ . The circuit diagram for the two principal experiments described in this report are shown in figure 1. The two circuits differed in that the bridge was balanced manually in one circuit and automatically by means of the continuous-balance amplifier and motor in the other. Because  $R_3 = R_4$ ,  $R_w = R_2$  when the bridge is balanced. After a change in pressure causes  $R_w$  to vary and the bridge to become unbalanced, balance is restored by changing the current to the bridge by means of  $R_1$ .

### CALIBRATION SYSTEM

#### Choice of System

The volume-ratio method could be used successfully because of the availability of a vacuum system that had the following desirable characteristics: a large volume, a low outgassing rate, and a low ultimate pressure.

The main calibration tank was a bell jar of large volume (68.5 cu ft). This volume permitted the use of small-volume tanks sufficiently large that their volumes could be measured to high accuracy while volume ratios large enough to create calibration tank pressures to a lower limit of  $10^{-4}$  Torr were maintained. The low outgassing rate ( $dp_g/dt = 4 \times 10^{-6}$  Torr/min) permitted measurements to the  $10^{-4}$  Torr pressure level without a prohibitive degree of pollution of the high-purity gases used in the experiments. The same advantage was provided by the low ultimate pressure  $p_0$  ( $3 \times 10^{-6}$  Torr) that was obtainable. The accuracies obtainable from such a system make it useful as a pressure standard to a lower limit of  $10^{-4}$  Torr.

## Principle of Operation

The calibration system is represented schematically in figure 2. The bell jar and small-volume tank are initially evacuated to the ultimate pressure  $p_0$  by the diffusion pump. A quantity of gas is then transferred from the gas supply to the small-volume tank, where the initial pressure  $p_{T,1}$  can be measured by a diaphragm gage. The bell jar is then closed off from the diffusion pump, an arbitrary amount of the test gas is transferred into the bell jar, and thereby a lower pressure  $p_{T,2}$  in the small-volume tank is created. The pressure in the bell jar may then be expressed as

$$p_{BJ} = \frac{(p_{T,1} - p_{T,2})v_T}{v_{BJ}} + p_0 + \frac{dp_g}{dt} \quad (3)$$

provided that the bell-jar wall temperature is equal to the small-volume-tank wall temperature. The effect of adsorption will be discussed, since equation (3) assumes that no adsorption takes place.

## Description of System

The main calibration tank is a 4-foot-diameter, 5-foot-high bell-shaped tank made of mild steel. Two ports provide for the insertion of experimental equipment; electrical connectors are provided through the base plate. The pumping system consists of a 100-liter-per-second mechanical pump and a 16-inch diffusion pump that provides a speed of 1000 liters per second at the mouth of the bell jar. Backstreaming of oil from the diffusion pump is kept to a minimum by means of a water-cooled baffle and a Z-section between the pump and the system. The system pumps from atmospheric pressure to the  $10^{-5}$  Torr level in about 20 minutes. The time required to attain the ultimate pressure of  $3 \times 10^{-6}$  Torr depends on the previous history of bell-jar exposure to atmospheric pressure, but it is normally on the order of 24 hours.

The small-volume tanks are constructed of stainless steel (tank A) and brass (tanks B and C). Connections are made with 1/4-inch-outside-diameter copper tubing, bellows-sealed valves, and soldered fittings.

Diaphragm-type absolute-pressure gages with ranges of 0 to 20 and 0 to 225 Torr were used to measure the pressure in the calibration tanks. A mechanical vacuum pump evacuated the gage case to a negligible pressure level to ensure correct absolute-pressure indication.

The test gases used in the experiments were argon, carbon dioxide, helium, and nitrogen of 99.9 percent purity as specified by the commercial source from which they were obtained.

## Experimental Procedure

A datum point or group of datum points was obtained in the following manner:

With the bell jar at the ultimate pressure of  $3 \times 10^{-6}$  Torr, the bridge was balanced and the current through the wire recorded; the pressure in the small-volume tank was measured. A quantity of gas was then transferred into the bell jar from the small-volume tank, the bridge was rebalanced, and the new current level and small-volume pressure were recorded. After this procedure was used through an arbitrary number of gas transferences, the bell jar was reevacuated and the zero-pressure current redetermined. Tank wall temperatures were recorded. The sensing element was mounted inside the vacuum system, and the gage wall temperature was recorded with a thermistor.

## RESULTS AND DISCUSSION

### Accuracy Considerations

Thermal-conductivity gage. - Table II lists the principal parameters involved in the heat-transfer relation of the wire, the random variation of the parameters, the effect of the random variation on the accuracy of the pressure measurement, and the method by which the parameters were measured or controlled.

The emittance of the wire was not directly measured, but the stability of this property can be inferred from the data presented in the section on reproducibility of results. A computation shows that a random variation in emittance of  $\pm 1$  percent would result in a random variation in the pressure measurement of  $\pm 60$  percent at  $10^{-4}$  Torr, when end losses are assumed negligible. An estimate of the end losses, based on an example presented by Leck (ref. 7, p. 61), was made in order to substantiate this assumption, with the result that end losses were found to be less than 10 percent of the radiation loss. Figure 3 illustrates why the radiation term has such a profound effect on the accuracy of the pressure measurement. At  $10^{-4}$  Torr the heat loss by radiation and end conduction represents 99 percent of the total heat loss from the wire, which justifies the necessity for the high accuracy of the measurements given in table II.

Calibration system. - The accuracy of the volume-ratio method depends upon the accuracy to which the various volumes are determined and on the accuracy of the diaphragm gage. Table III indicates the volume of the components, the limit of error of these measurements, and the technique used to determine the volume. The degree of precision of each measurement is compatible with the contribution of the component to the total volume of the system.

It can be seen from table III that three sizes of small-volume tanks and two diaphragm gages with different ranges of pressure were used in the experiments. These tanks and gages were interchangeable and were used in different combinations. The tank-gage combinations used are tabulated in figure 4, which shows the effect of the accuracy of the diaphragm gages on the accuracy of the volume-ratio method; the figure is based on the fact that the limit of error of the diaphragm gages is  $\pm 0.3$  percent of maximum pressure value. Note that the pressure created by any tank-gage combination reaches a maximum limit of error of about 3 percent before it is overlapped by another tank-gage combination that can produce that pressure more accurately; an exception exists below  $2 \times 10^{-4}$  Torr where the limit of error increases linearly to 6 percent at  $10^{-4}$  Torr.

The effect of the volume measurements on the accuracy of the calibration system can be determined from table III. The accuracy of each small-volume-tank measurement can be obtained by an algebraic summation of the volumes and limits of error of the components involved; that is, the tank itself, the connecting tubulation, the internal volume of the diaphragm gage, and the change in the volume of the diaphragm with pressure are added together to obtain the total volume of the small-volume tank. Calculation shows the maximum limit of error of any volume measurement to be less than 1 percent. Thus, an error analysis of the entire calibration system (i.e., diaphragm-gage error and volume error) shows that the diaphragm-gage error predominates, and therefore the limit of error values given herein essentially applies for the calibration system as a whole.

The volume-ratio calibration system was compared with an independent pressure measurement. A dibutyl phthalate manometer, read with a cathetometer to an accuracy of  $\pm 5 \times 10^{-3}$  Torr, was connected to the bell jar. Gas was transferred into the bell jar a number of times from small-volume tank C until the bell-jar pressure level was so high as to render the uncertainty of the manometer negligible. The two methods agreed to within 0.7 percent at 4 Torr. The test, however, only verified the accuracy of the volume determination of tank C. Tanks A and B were then compared with tank C to give an indirect comparison against the manometer.

#### Reproducibility of Results

The heat-transfer equation for the wire when the bell jar is at essentially zero pressure is

$$i_0^2 R_w = Q_{\text{rad}} + Q_{\text{end}} \quad (4)$$

At a finite pressure level, still in the free molecular region, equation (2) holds true. Assuming that  $Q_{\text{rad}}$  and  $Q_{\text{end}}$  remain constant as pressure changes and subtracting equation (4) from equation (2) give

$$i^2 - i_0^2 = \alpha \left( \frac{\gamma + 1}{\gamma - 1} \right) \sqrt{\frac{R}{T_a M}} A_s \frac{T_w - T_a}{R_w} p \quad (5)$$

Figure 5 is a graph of output signal  $i^2 - i_0^2$  against pressure for nitrogen in the range of  $10^{-4}$  to 1 Torr. The curve is divided into two ranges, range 1 from  $10^{-4}$  to  $1.5 \times 10^{-3}$  Torr and range 2 from  $5 \times 10^{-3}$  to 1 Torr. The wire operating conditions for the two ranges are given in table IV. Equation (5) has been used to normalize the data of range 2 to the wire- and ambient-temperature values of range 1, which results in the same straight line through both sets of data. This normalizing technique is discussed in the next section.

The straight line drawn through the data (data points are not shown because of the scale of the graph) represents the theoretical free-molecule heat transfer according to equation (5), with the value of the accommodation coefficient chosen that causes the line to best fit the data. The same value of accommodation coefficient was chosen for the data of both range 1 and range 2. The data begin to



deviate from this line at about  $5 \times 10^{-2}$  Torr, which is indicative of the boundary between the free-molecule and slip regions. This deviation can be seen more clearly in figure 6(a). Figure 6(a) presents the data of range 2 in the form  $(p' - p)/p$  plotted against  $p$ , where  $p'$  is the pressure indicated by the thermal-conductivity gage and  $p$  the pressure as represented by the theoretical straight line. This figure shows the average deviation from the mean curve to be about 1 percent throughout most of range 2; it also shows the deviation from free-molecule theory to begin, as previously mentioned, at about  $5 \times 10^{-2}$  Torr, which amounts to 5 percent deviation in pressure indication at about  $3 \times 10^{-1}$  Torr and 10 percent at about  $5.5 \times 10^{-1}$  Torr. Figure 6(b) presents the data of range 1 and shows the average deviation from the mean curve to be about 2 percent.

#### Effect of Variation in Ambient and Wire Temperatures

The need for accurate control of ambient and wire temperatures is demonstrated in figure 7. The graph illustrates the uncertainty in pressure indication that would occur if the temperatures were subjected to a random variation of  $\pm 0.1^\circ$  F. The result would be a  $\pm 3$  percent uncertainty in pressure indication at  $10^{-4}$  Torr due to a  $\pm 0.1^\circ$  F random variation in ambient temperature (fig. 7(a)) and a  $\pm 7$  percent uncertainty in pressure indication at  $10^{-4}$  Torr for a  $\pm 0.1^\circ$  F random variation in wire temperature (fig. 7(b)).

The effect of a systematic change in ambient or wire temperature is shown in figure 8. The solid curve is the range 1 curve of figure 5. The dashed curve is the curve of output signal  $i^2 - i_0^2$  plotted against pressure for a  $10^\circ$  F increase in wire temperature from the range 1 curve value; the dash-dot curve is the curve of  $i^2 - i_0^2$  plotted against pressure for a  $10^\circ$  F increase in ambient temperature from the range 1 curve value. These curves were generated by inserting the appropriate temperature values in equation (5). Thus, once a calibration curve is established for a particular set of values of ambient and wire temperatures, data obtained at slightly different temperature levels can be normalized to the original calibration curve. This technique is useful in the field, where slightly different temperature environments might exist. It was employed to normalize the data of range 2 to the temperature values of range 1.

While the method of presenting the data in a plot of  $i^2 - i_0^2$  against pressure has the advantage of a linear calibration in the free-molecule region, it does require a knowledge of the current at the ultimate pressure level  $i_0$ . This knowledge is not possible in all vacuum systems. The purpose of a periodic check of  $i_0$  is to verify that the emittance of the wire has remained within the specified limits ( $\pm 0.1$  percent for the data of this report).

The operation of the gage would be simplified by eliminating the systematic changes in ambient temperature. The required degree of control of ambient temperature ( $\pm 0.05^\circ$  F) can be obtained from commercially available constant-temperature electric ovens. Preliminary data taken with such devices have shown results comparable to the data presented herein.

Situations outside the realm of the application of this gage are systems in which gas composition is unknown and temperature or pressure environments are rapidly fluctuating. The gage, however, does bring more accuracy and flexibility to the problem of providing measurement standardization, especially in the lower decades of the range discussed in this report. This range has always been a borderline region for a number of vacuum gages.

#### Calibration with Various Gases

Experimental data were obtained with nitrogen, argon, carbon dioxide, and helium. Equation (5) was then fitted to the experimental data by choosing the appropriate accommodation coefficient. The values of the coefficient thus obtained are presented in table V. Also included are the results obtained by Amdur and Guildner (ref. 8) for the accommodation coefficients of various gases on an unflashed tungsten wire. Both results are for a wire temperature of approximately 250° F. The data indicate that the surface conditions of the wires are very similar. This similarity suggests that the data of reference 8 could be used to draw calibration curves for those gases not covered by this investigation, and the necessity of experimental determination of each accommodation coefficient eliminated. It is felt that this technique could be utilized for those applications where accuracies of  $\pm 5$  percent were acceptable, since the agreement between accommodation coefficient values obtained in both experiments is within this limit.

The calibration curves for these other gases can be drawn as a straight line to about  $10^{-1}$  Torr, where slip-flow effects are still negligible (see fig. 6(a)). This has been done in figure 9 for the experimentally determined curves and the curves based on the accommodation coefficient values of reference 8. For accurate calibration no further extension of the curves on the basis of free-molecule theory should be attempted beyond about  $3 \times 10^{-1}$  Torr, where slip flow effects are responsible for a 5-percent change in pressure indication for the experimental data.

Note that, for any given gage output signal, the pressure ratio for two different gases is a constant. Thus, the following table of the ratio of the gas pressure to nitrogen pressure  $p/p_{N_2}$  presents each gas as a constant multiple of the nitrogen calibration curve:

Gas	$p/p_{N_2}$
Hydrogen	0.66
Carbon dioxide	0.94
Nitrogen	1.00
Oxygen	1.02
Helium	1.05
Neon	1.38
Argon	1.61
Krypton	2.31
Xenon	2.83

## Effect of Contaminants

An attempt was made to change the calibration of the wire by exposing it to vapors that are commonly present as contaminants in vacuum systems. If it were proved that the wire surface is highly sensitive to these impurities, extreme care would be necessary to keep the gage in a spotless condition.

The gage was first exposed to vapors of water, acetone, and carbon tetrachloride for 24 hours each at a pressure of about 5 Torr. The gage was operated at its normal wire temperature. The gage was then recalibrated in nitrogen; no change in calibration was observed. Next the gage was placed in a small vacuum system that contained a pool of mechanical pump oil. The oil was heated to 125° F, which corresponds to a vapor pressure of  $5 \times 10^{-1}$  to 1 Torr. The system was then pumped to well below this pressure ( $2.5 \times 10^{-2}$  Torr) to ensure an atmosphere of hot oil vapor in the system. The gage was operated in this atmosphere for 24 hours, then exposed to normal atmospheric air pressure for 24 hours, and finally for 24 hours more in the hot oil vapor. The gage was then recalibrated in nitrogen (without any cleaning of the gage tube or wire), and no shift in calibration was observed. The only effect on the wire was to cause an apparent change in emittance of about 2 percent as evidenced by the change in the current at the ultimate pressure. Since the radiation term is eliminated from the heat-transfer equation (5), this result had no effect on the calibration of the gage. It may also be concluded that no complications will arise from contamination effects because the wire showed no aging effects during the entire experimental time (30 months).

## Effect of Adsorption

The volume-ratio method has been applied in this investigation with the assumption that a negligible amount of the gas that is transferred into the bell jar is adsorbed at the walls. If this assumption were not true and a significant amount of adsorption occurred, the actual pressure in the bell jar would be lower than that predicted by the calibration system by an amount directly proportional to the percentage of the gas adsorbed.

The linear relation between the output of the thermal-conductivity gage (in the form  $i^2 - i_0^2$ ) and the pressure as predicted by the calibration system can be used to determine the degree of adsorption. This proof is based on the assumptions that there is a maximum adsorptive capacity of the walls and that this maximum quantity of gas is adsorbed almost instantaneously. The experimental data to validate these assumptions are given in reference 9.

If, for example, a quantity of gas sufficient to raise the pressure to  $10^{-4}$  Torr were transferred into the bell jar and the thermal-conductivity gage continued to read zero pressure, it would be immediately obvious that the entire volume of gas had been adsorbed at the walls (or that the valve to the diffusion pump had been left open). As more gas is transferred into the bell jar, the adsorptive capacity of the walls would eventually be reached and the thermal conductivity gage would begin to indicate a finite pressure level. The resulting relation between  $i^2 - i_0^2$  and pressure as computed from the volume-ratio method

would be nonlinear. Analysis of figure 6(b) shows that no nonlinearity occurred even at the lowest pressure level of  $10^{-4}$  Torr. The scatter of the data, about  $\pm 3$  percent, indicates that the degree of adsorption is at least less than about 3 percent at the low pressure limit of the experiments.

#### SUMMARY OF RESULTS

The volume-ratio calibration system described herein is a convenient method to use as a primary standard to a lower pressure limit of  $10^{-4}$  Torr. An error analysis showed that the pressures could be produced with a limit of error of about 3 percent to a lower limit of  $2 \times 10^{-4}$  Torr, and increased linearly to about 6 percent at  $10^{-4}$  Torr.

The thermal-conductivity gage was tested in the range  $10^{-4}$  to 1 Torr. The data obtained were reproducible to  $\pm 1$  percent in the range  $5 \times 10^{-3}$  to 1 Torr and to  $\pm 2$  percent in the range  $10^{-4}$  to  $1.5 \times 10^{-3}$  Torr. The accuracy was obtained only by use of very high quality secondary instrumentation obtainable in the laboratory but not always available for field operations. Also, the ability to make frequent references to the zero-pressure current level made it possible to verify the stability of the emittance of the gage wire within the specified limits.

Calibration curves were obtained experimentally for helium, nitrogen, argon, and carbon dioxide, while suggested curves for hydrogen, neon, oxygen, krypton, and xenon were obtained on the basis of an accommodation-coefficient comparison.

Attempts to contaminate the gage with substances commonly found in vacuum systems showed negligible effects on the calibration of the gage. The gage wire showed no appreciable aging effects during 30 months of operation.

It was suggested that the operation of the gage could be simplified by replacing the ambient-temperature-correction technique with a constant-temperature electric oven. This replacement would allow direct conversion of the output signal into its pressure equivalent without the necessity of first applying corrections due to temperature changes. Preliminary data obtained with such a device indicated this conclusion to be valid. Certain situations of unknown gas composition, continuous temperature variations within a vacuum system, or a rapid fluctuation of pressure would be outside the realm of the application of this gage. But the gage did allow more accuracy and flexibility with which to provide measurement standardization to the growing number of vacuum applications.

Lewis Research Center

National Aeronautics and Space Administration  
Cleveland, Ohio, March 13, 1963

## APPENDIX - SYMBOLS

A	area
i	current
k	thermal conductivity
M	molecular weight
p	pressure
p'	pressure indicated by thermal-conductivity gage
$Q_{\text{cond}}$	heat-flow rate from wire to end supports
$Q_{\text{gas}}$	heat-flow rate from wire to gas
$Q_{\text{in}}$	heat-flow rate into wire
$Q_{\text{rad}}$	heat-flow rate from wire by radiation
R	resistance
$\mathcal{R}$	universal gas constant
T	temperature
t	time
v	volume
x	distance along wire
$\alpha$	accommodation coefficient
$\epsilon$	emittance
$\sigma$	Stefan-Boltzmann constant
$\gamma$	ratio of specific heats, $c_p/c_v$

### Subscripts:

O	conditions with vacuum system at ultimate pressure
a	ambient
BJ	bell jar (main calibration tank)
cs	cross section

end    ends of wire  
g      outgassing  
s      surface  
T      small-volume tank  
w      wire

## REFERENCES

1. Brombacher, W. G.: Bibliography and Index on Vacuum and Low Pressure Measurement. Monograph 35, NBS, 1961.
2. Fryburg, G. C., and Simons, J. H.: A Precision Vacuum Gage. Rev. Sci. Instr., vol. 20., no. 8, Aug. 1949, pp. 541-548.
3. Alpert, D.: New Developments in the Production and Measurement of Ultra High Vacuum. Jour. Appl. Phys., vol. 24, no. 7, July 1953, pp. 860-876.
4. Flanick, A. P., and Ainsworth, J.: A Thermistor Pressure Gage. NASA TN D-504, 1960.
5. Schuhmann, S.: Application of Knudsen's Method of Pressure Division to the Calibration of Vacuum Gages. Paper Presented at Ninth Symposium of Am. Vacuum Soc., Los Angeles (Calif.), Oct. 31 - Nov. 2, 1962.
6. Dushman, S., and Lafferty, J. M.: Scientific Foundations of Vacuum Technique. Second ed., John Wiley & Sons, Inc., 1962.
7. Leck, J. H.: Pressure Measurements in Vacuum Systems. Inst. Phys., Chapman and Hall, Ltd. (London), 1957.
8. Amdur, I., and Guildner, L. A.: Thermal Accommodation Coefficients on Gas-Covered Tungsten, Nickel and Platinum. Jour. Am. Chem. Soc., vol. 79, no. 2, Jan. 20, 1957, pp. 311-315.
9. Lee, D., Tomaschke, H., and Alpert, D.: Adsorption of Molecular Gases on Surfaces and Its Effect on Pressure Measurement. Rep. I-104, Coordinated Sci. Lab., Univ. Ill., Aug. 1961.

TABLE I. - CHARACTERISTICS OF GAGE SENSING ELEMENT

Wire material . . . . .	Aged tungsten
Wire geometry . . . . .	Helix
Helix pitch, in. . . . .	0.0045
Helix diameter, in. . . . .	0.0015
Resistance at 0° C, ohms . . . . .	77.0
Diameter, in. . . . .	0.0005
Extended length, in. . . . .	4.6
Surface area, sq in. . . . .	0.007
Total emittance <sup>a</sup> . . . . .	0.13
I.D. of surrounding glass envelope, in. . . . .	3/16

<sup>a</sup>Determined from experimental results.

TABLE II. - RANDOM VARIATION OF GAGE PARAMETERS

Parameter	Controlling or measuring instrument	Random variation		Effect of random variation on accuracy of pressure measurement	
		°F	percent	percent	Measured at - Torr
Manual control; pressure range, $5 \times 10^{-3}$ to 1 Torr					
Current	Potentiometer and 10 ohm shunt	----	±0.3	±1	$5 \times 10^{-3}$
Ambient temperature	Thermocouple	±0.3	----	±.1	$5 \times 10^{-2}$
Wire temperature	Manual control of circuit current	±.1	----	±.2	$5 \times 10^{-3}$
Emittance	Inferred from data	----	<±.1	±.3	$5 \times 10^{-3}$
Automatic control; pressure range, $10^{-4}$ to $1.5 \times 10^{-3}$ Torr					
Current	Digital voltmeter and 1500 ohm shunt	----	±0.1	±2	$10^{-4}$
Ambient temperature	Thermistor	±0.05	----	±.2	$10^{-3}$
Wire temperature	Amplifier and balancing motor	±.02	----	±1.5	$10^{-4}$
Emittance	Inferred from data	----	<±.1	±2	$10^{-4}$



TABLE III. - CALIBRATION-SYSTEM VOLUMES

Component	Volume, cu in.	Method of determination
Small volume tank:		Weight of water
A	12.35±0.03	
B	27.00±0.07	
C	294.7±0.7	
Main calibration tank (bell jar)	<sup>a</sup> 68.5±0.6	Independent volume ratio
Connecting tubulation	1.57±0.05	Geometric measurement
Diaphragm-pressure- gage capsule <sup>b</sup> and internal tubulation		Volume ratio
0 to 225 Torr gage	0.75±0.02	
0 to 20 Torr gage	0.29±0.02	
Volume change of gage capsule <sup>c</sup>		Gas displacement
0 to 225 Torr	0.28±0.02	
0 to 20 Torr	0.065±0.005	

<sup>a</sup>Measured in cu ft.<sup>b</sup>At pressure of zero.<sup>c</sup>Zero to maximum pressure.

TABLE IV. - EXPERIMENTAL OPERATING CONDITIONS

Parameter	<sup>a</sup> Range 1	<sup>b</sup> Range 2
Wire resistance, ohms	122	127
Wire temperature, °F	242	266
Ambient temperature, °F	74±4	80±4
Experimental runs	9	20
Data points	73	175
Approximate current at zero pressure, ma	2	2
Approximate current at 10 <sup>-2</sup> Torr, ma	---	3
Approximate current at 5×10 <sup>-1</sup> Torr, ma	---	15

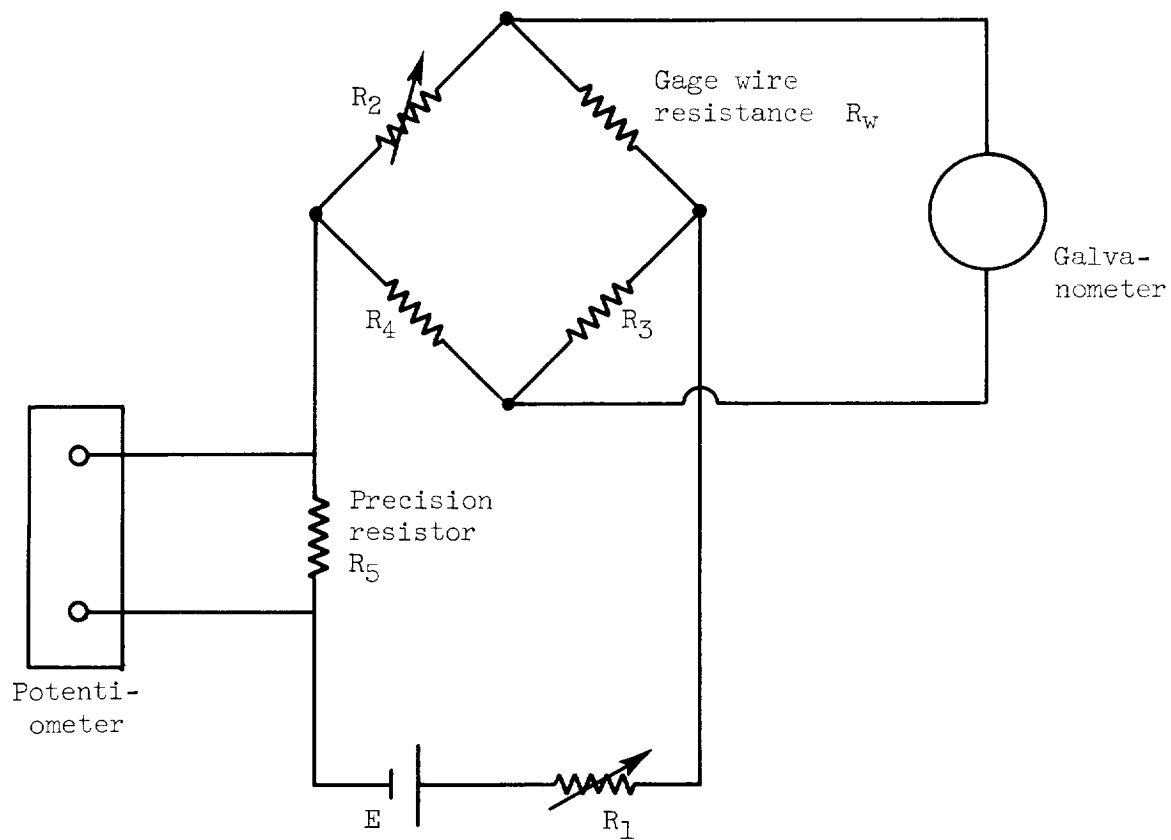
<sup>a</sup>10<sup>-4</sup> to 1.5×10<sup>-3</sup> Torr.<sup>b</sup>5×10<sup>-3</sup> to 1 Torr.

TABLE V. - COMPARISON OF ACCOMMODATION COEFFICIENTS

OF REFERENCE 8 AND THIS INVESTIGATION OBTAINED

AT WIRE TEMPERATURE OF APPROXIMATELY 250° F

Gas	Accommodation coefficients	
	Reference 8	Present investigation
Hydrogen	0.36	----
Helium	.48	0.48
Neon	.80	----
Nitrogen	.85	.89
Oxygen	.89	----
Argon	.99	.97
Krypton	1.00	----
Xenon	1.00	----
Carbon dioxide	----	.91

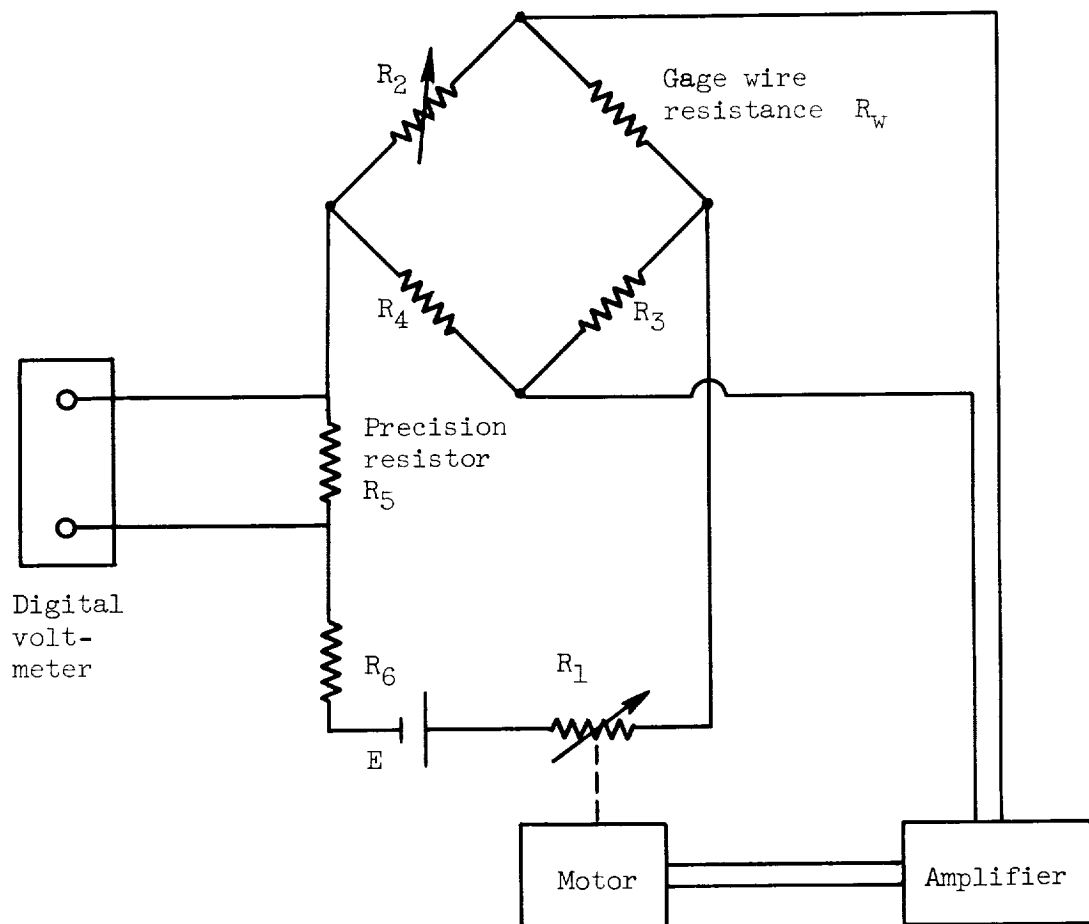


Values of circuit components

$R_W \cong 120$ ohms	$R_4 = 500$ ohms	Galvanometer:
$R_1 = 0-2000$ ohms	$R_5 = 10$ ohms	Coil resistance, 31 ohms
$R_2 = R_W$	$E \cong 3$ volts	Sensitivity, $0.15 \mu\text{a/mm}$
$R_3 = 500$ ohms		

(a) Manual control.

Figure 1. - Circuit diagram for thermal-conductivity gage.



#### Values of circuit components

$R_W \cong 120$  ohms  
 $R_1 = 0-1000$  ohms  
 $R_2 = R_W$   
 $R_3 = 100$  ohms

$R_4 = 100$  ohms  
 $R_5 = 1500$  ohms  
 $R_6 \cong 15,000$  ohms  
 $E \cong 45$  volts

Amplifier and motor:  
 Dead zone,  $\pm 2$  microvolts  
 Motor speed, approximately 20  
 seconds for 15 turns of  $R_1$   
 (0 to maximum value)

(b) Automatic control.

Figure 1. - Concluded. Circuit diagram for thermal-conductivity gage.

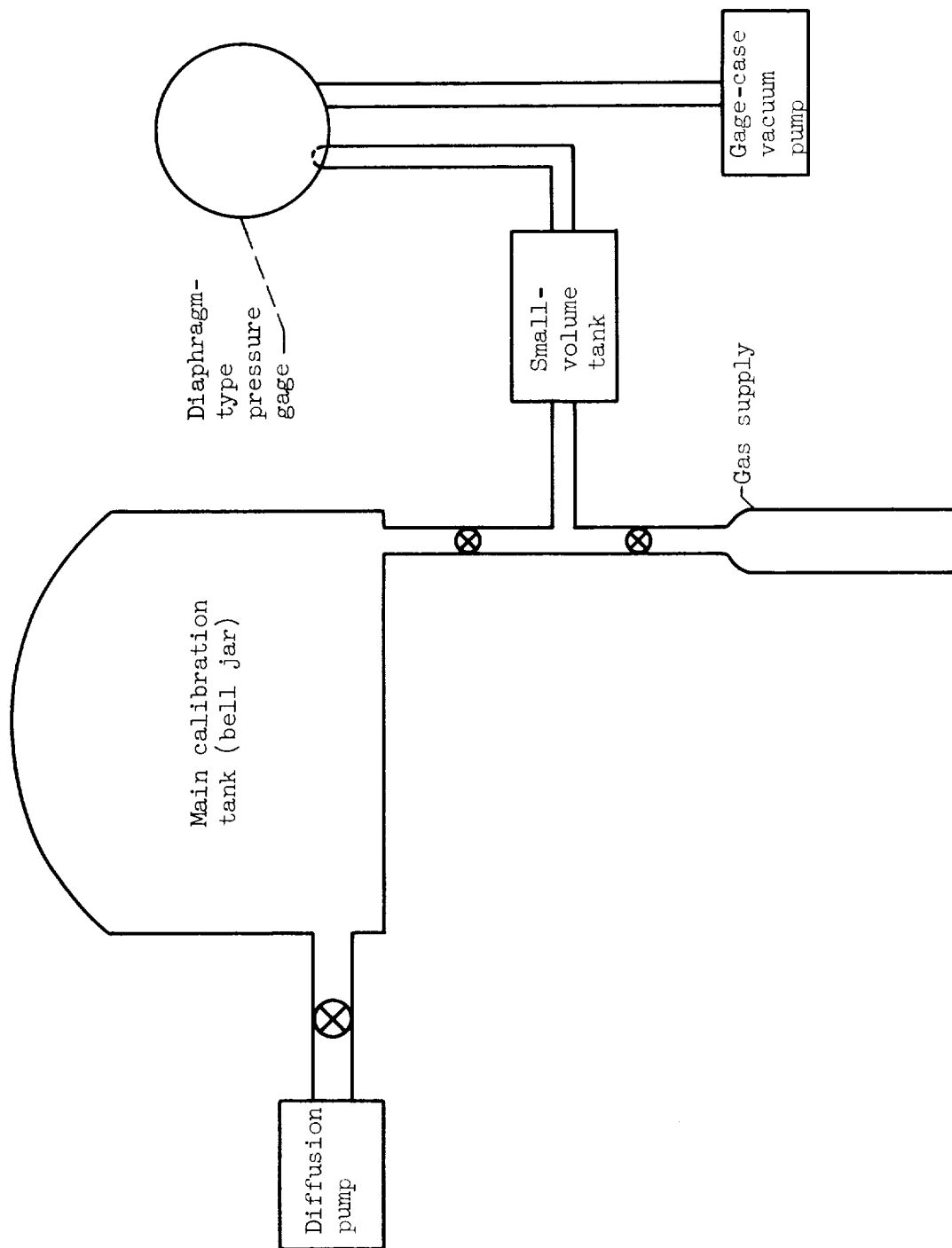


Figure 2. - Volume-ratio calibration facility.

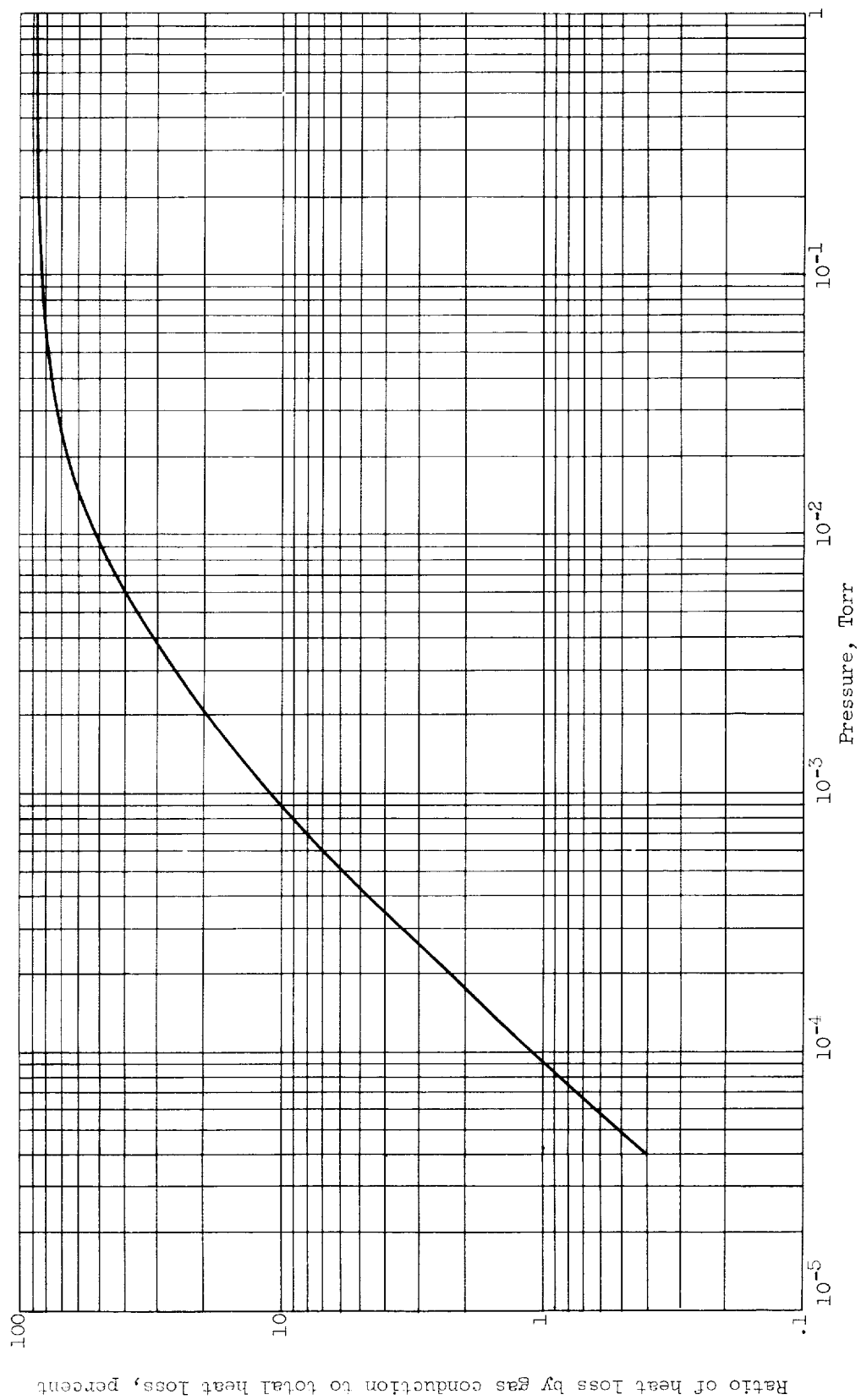


Figure 3. - Ratio of heat loss by gas conduction to total heat loss from thermal-conductivity gage obtained at various pressures.

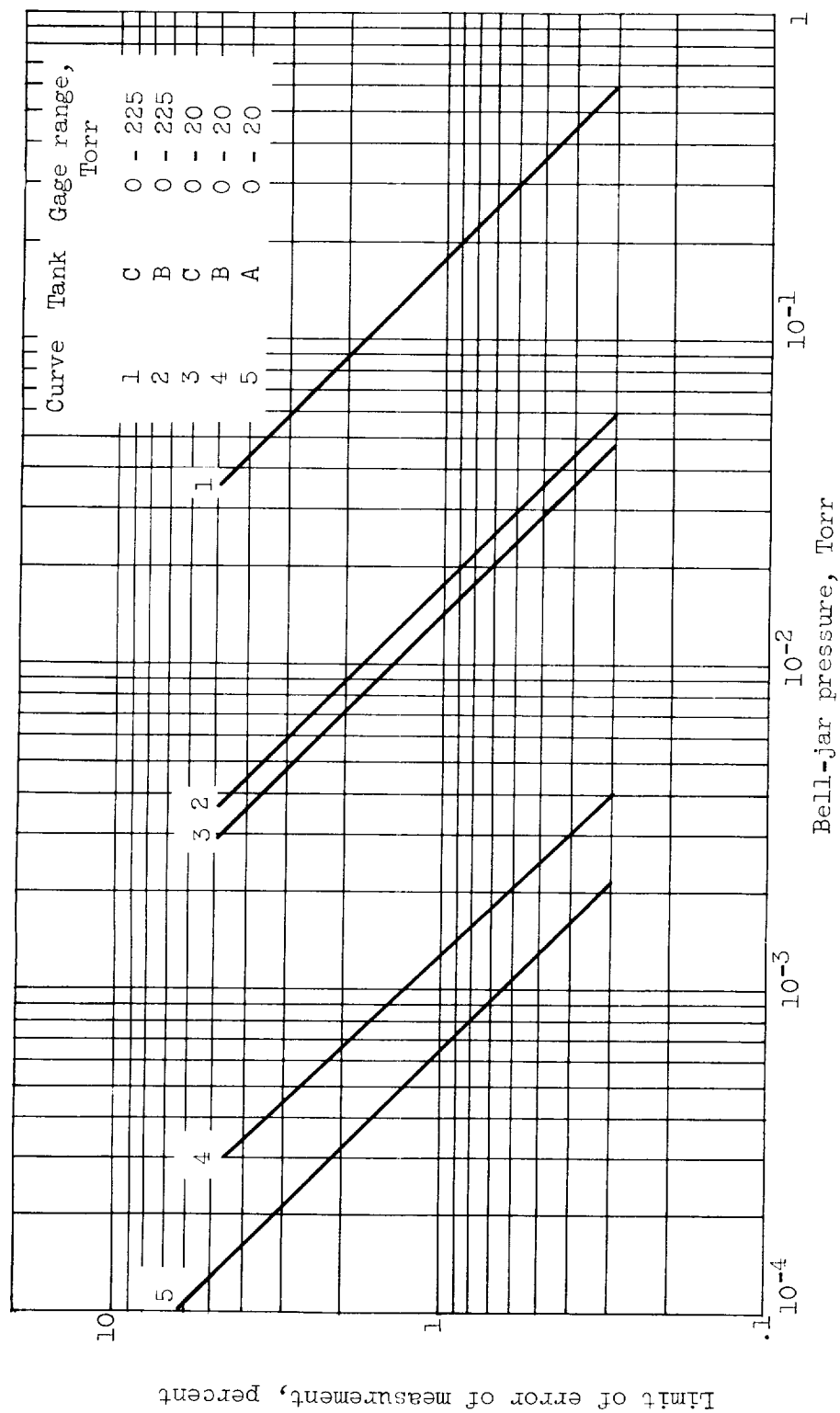


Figure 4. - Effect of accuracy of diaphragm gages on accuracy of volume-ratio method.

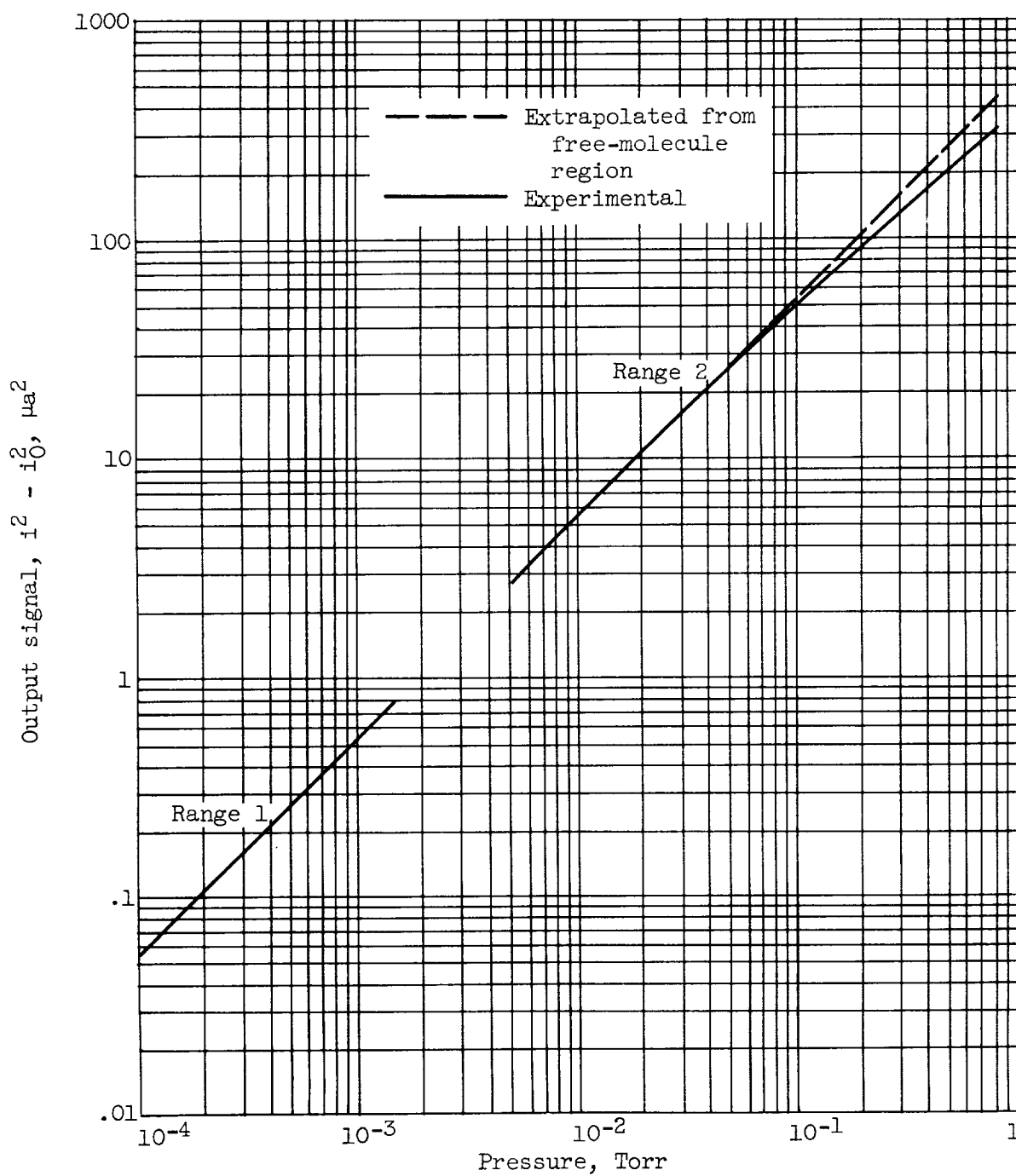


Figure 5. - Variation in output signal with pressure for thermal-conductivity gage. Test gas, nitrogen.



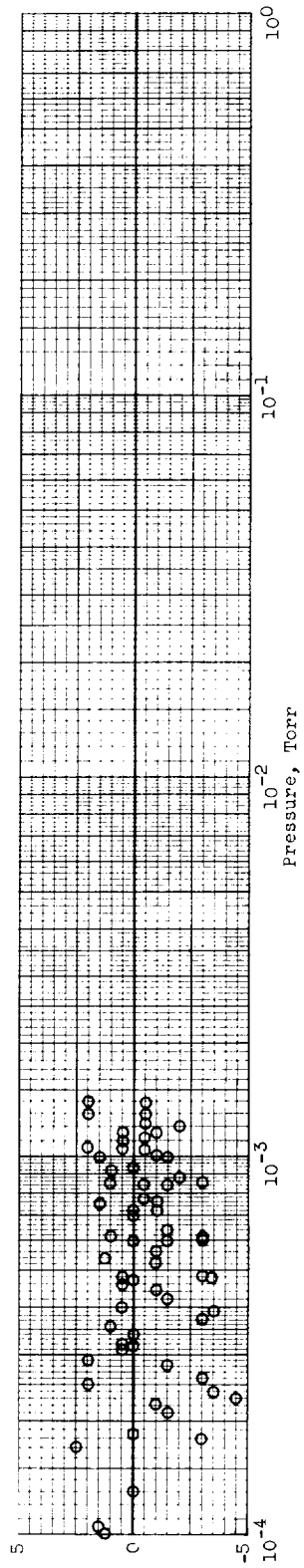
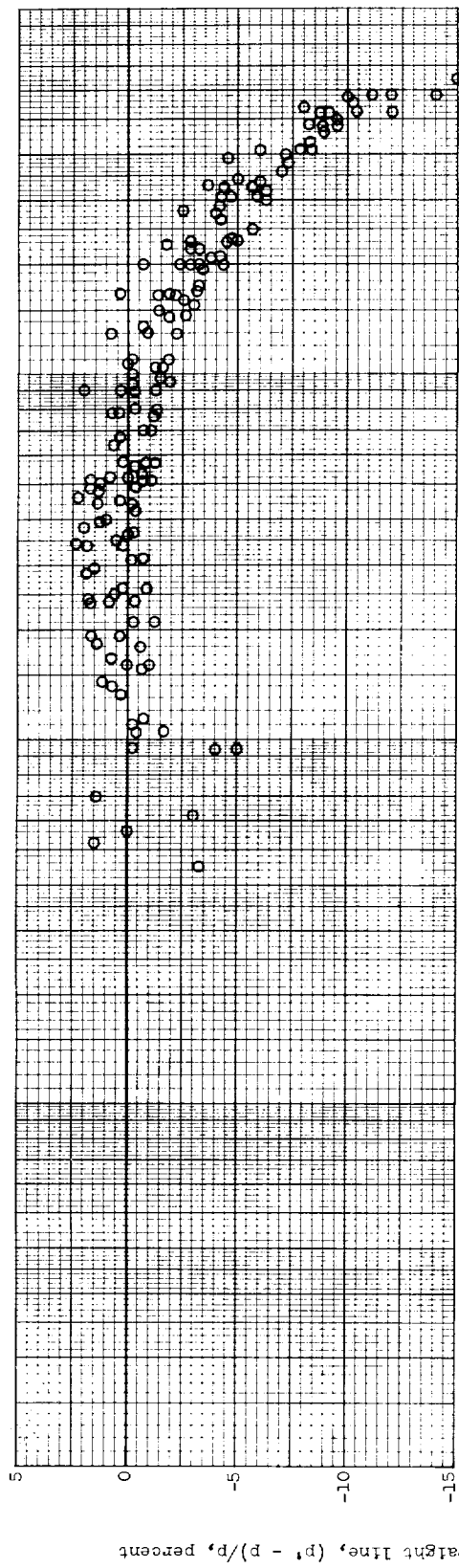
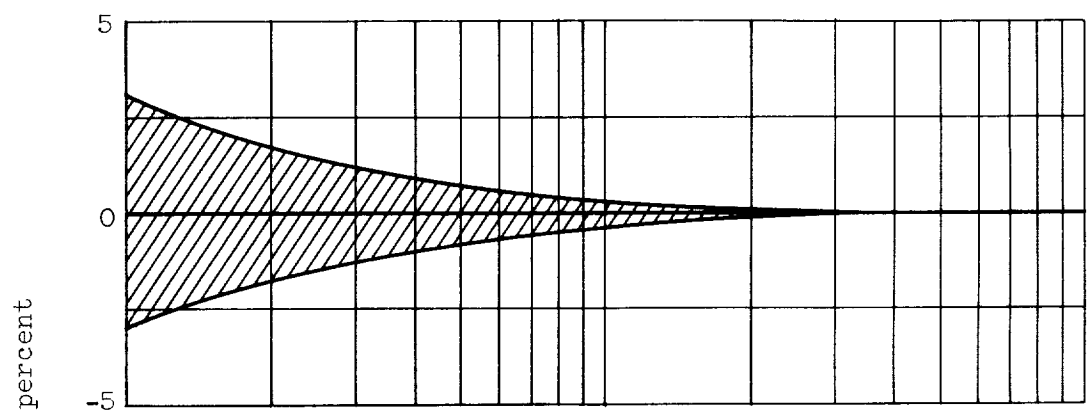
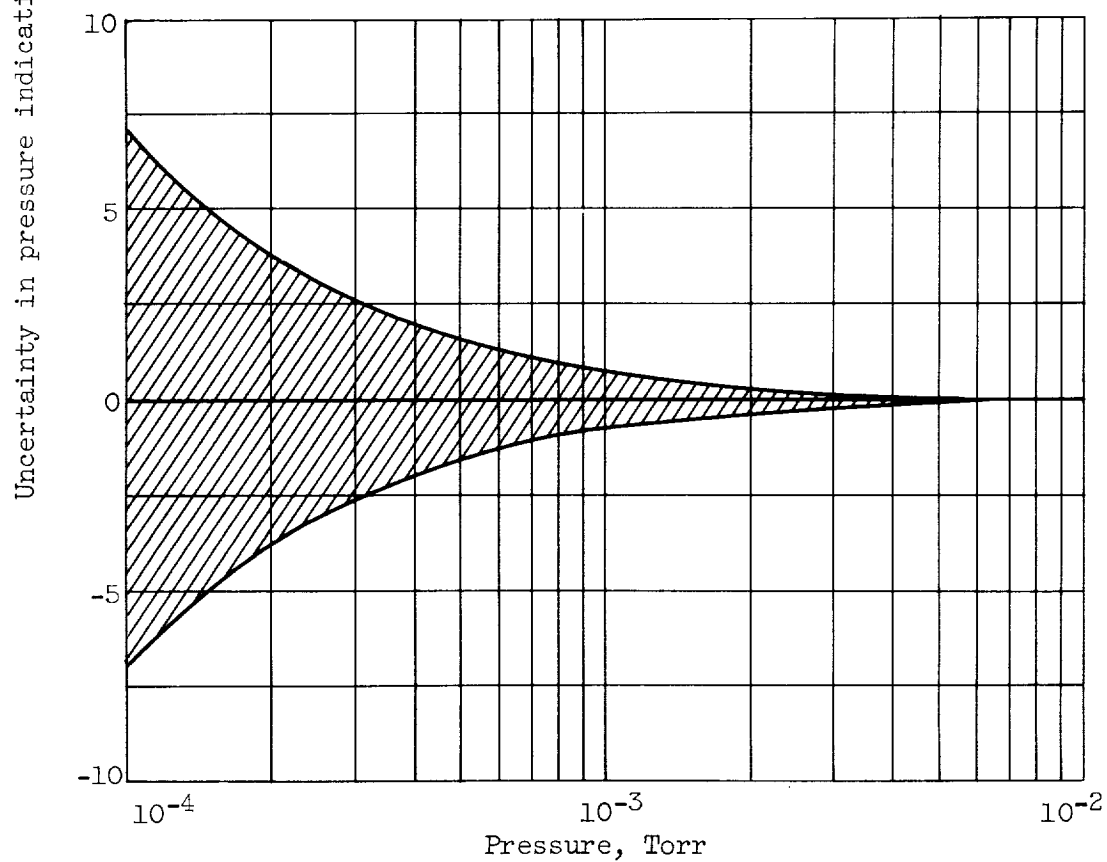


Figure 6. - Calibration of thermal-conductivity gage with nitrogen.



(a) Ambient temperature variation,  $\pm 0.1^\circ \text{ F}$ .



(b) Wall temperature variation,  $\pm 0.1^\circ \text{ F}$ .

Figure 7. - Effect of random temperature variation on pressure indication.

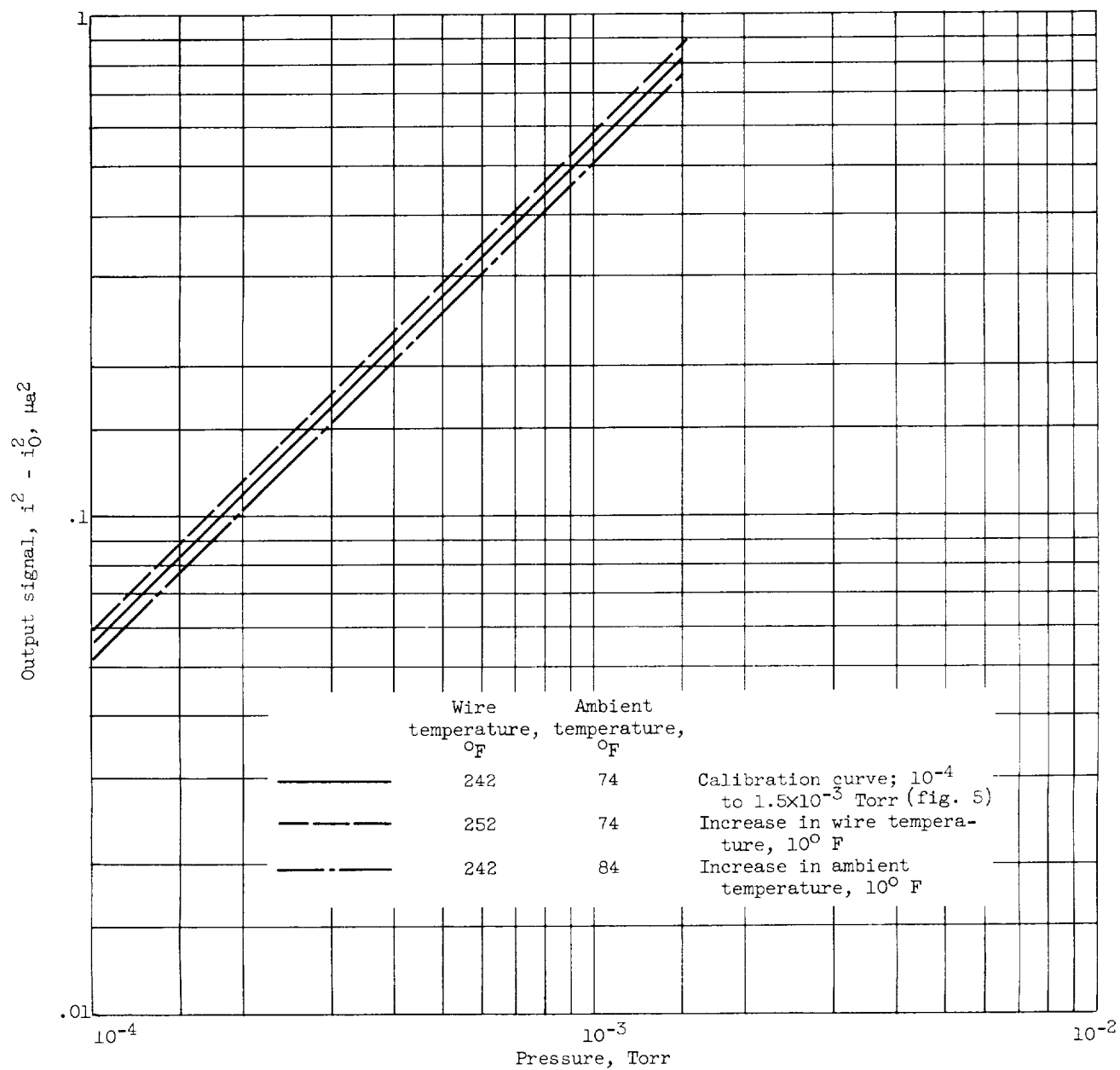


Figure 8. - Effect of systematic change in ambient or wire temperature on gage calibration curve.

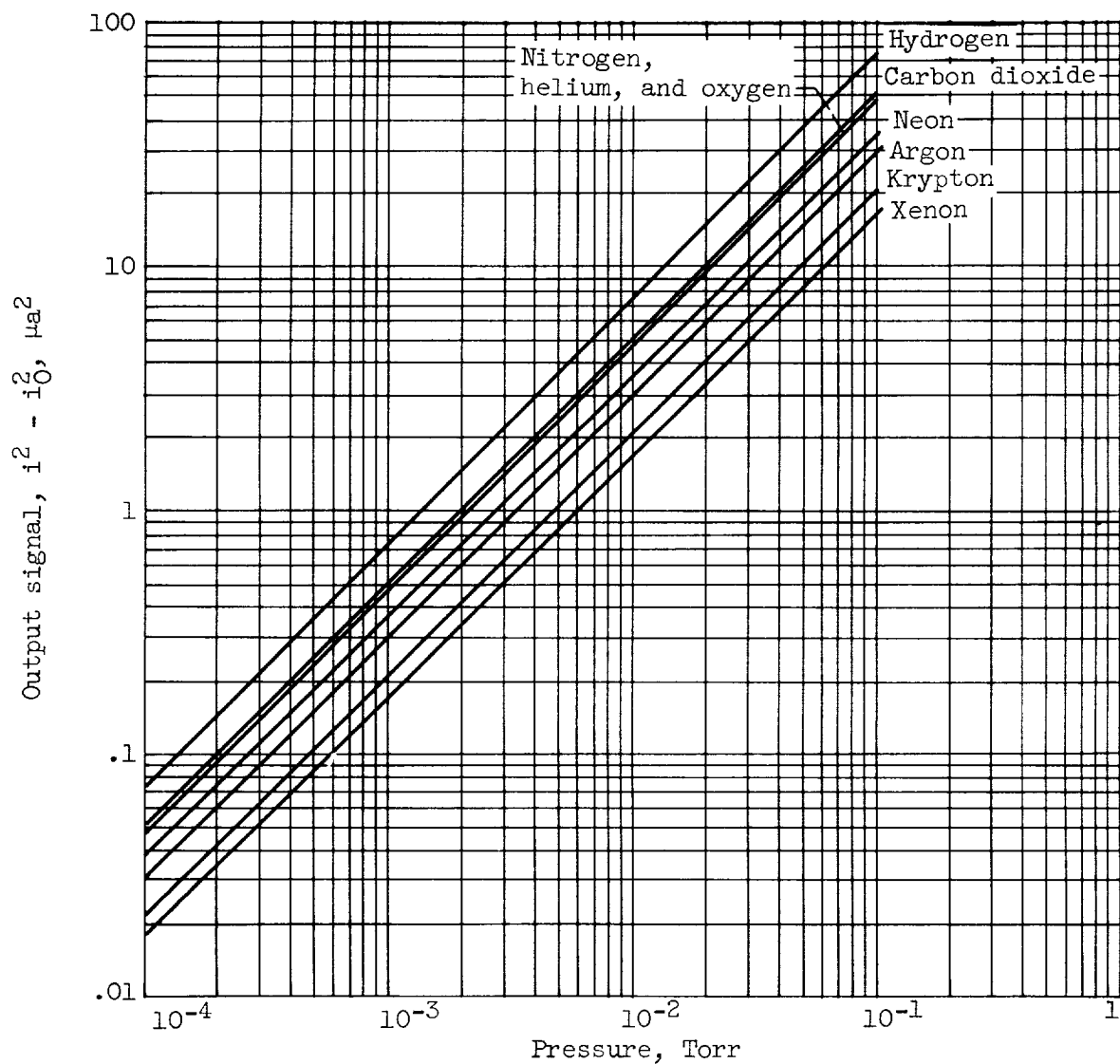


Figure 9. - Calibration curves for various gases with thermal-conductivity gage. Curves determined experimentally for carbon dioxide, helium, nitrogen, and argon; curves determined from accommodation coefficients of reference 8 for hydrogen, oxygen, neon, krypton, and xenon.